

Evidence of an asteroid encountering a pulsar

P. R. Brook¹ and A. Karastergiou

Astrophysics, University of Oxford, Denys Wilkinson Building, Keble Road, Oxford OX1 3RH, UK

paul.brook@astro.ox.ac.uk

S. Buchner²

Hartebeesthoek Radio Astronomy Observatory, P.O. Box 443, Krugersdorp, 1740, South Africa

S. J. Roberts

Information Engineering, University of Oxford, Parks Road, Oxford OX1 3PJ, UK

M. J. Keith³, S. Johnston and R.M. Shannon

CSIRO Astronomy & Space Science, Australia Telescope National Facility, P.O. Box 76, Epping, NSW 1710, Australia

ABSTRACT

Debris disks and asteroid belts are expected to form around young pulsars due to fallback material from their original supernova explosions. Disk material may migrate inwards and interact with a pulsar's magnetosphere, causing changes in torque and emission. Long term monitoring of PSR J0738–4042 reveals both effects. The pulse shape changes multiple times between 1988 and 2012. The torque, inferred via the derivative of the rotational period, changes abruptly from September 2005. This change is accompanied by an emergent radio component that drifts with respect to the rest of the pulse. No known intrinsic pulsar processes can explain these timing and radio emission signatures. The data lead us to postulate that we are witnessing an encounter with an asteroid or in-falling debris from a disk.

¹CSIRO Astronomy & Space Science, Australia Telescope National Facility, P.O. Box 76, Epping, NSW 1710, Australia

²School of Physics, University of Witwatersrand, Johannesburg, South Africa

³Jodrell Bank Centre for Astrophysics, School of Physics and Astronomy, University of Manchester, Manchester M13 9PL, UK

Subject headings: pulsars: general — pulsars: individual (PSR J0738-4042) — stars: neutron

1. Introduction

Pulsars are used as unique high-precision clocks in experimental astrophysics, primarily because of two fundamental characteristics. First, the average shape of the emitted radio beam (known as the pulse profile) remains remarkably stable over decades of observation, despite substantial variability from pulse to pulse. Second, the high moment of inertia and fast rotation of neutron stars results in extreme rotational stability, which can be measured by exploiting the stable pulse profile. The rotational frequency ν of all pulsars is gradually decreasing due to the loss of energy from magnetic dipole radiation. The time derivative of the frequency is known as the spin-down rate $\dot{\nu}$. The stability of pulsars allows timing models to account for phenomena that affect the arrival times of pulses on Earth, including relative motions, propagation effects, and general relativistic effects (Edwards et al. 2006).

In the last few years, evidence has been emerging that challenges both of the characteristics above. A small number of pulsars have been identified (Lyne et al. 2010), in which the average pulse profile switches between states on long timescales, some pulsars also showing a correlated change in $\dot{\nu}$. A similar but extreme example of variability is observed in a group of intermittent pulsars which go through a quasi-periodic cycle of switching on and off, on timescales of months to years (Kramer et al. 2006; Camilo et al. 2012; Lorimer et al. 2012). In these objects, each of their two states is associated with a different spin-down rate. In both cases of state-switching pulsars, the changes in $\dot{\nu}$ and emission have been attributed to the torque induced on the neutron star by changing magnetospheric currents (Timokhin 2010).

Neutron star glitches, characterized by a discrete increase and gradual relaxation of the rotational frequency, have also recently been linked to pulse profile variability in radio pulsars (Weltevrede et al. 2011; Keith et al. 2013). Further examples of glitches and irregular spin-down properties, associated with emission variability, have been seen in magnetars (Woods & Thompson 2006), where dramatic profile changes, related to changes in the magnetic field structure have been observed both in X-rays and radio (e.g. Camilo et al. 2007).

Profile and timing variability reduce the potential to use particular pulsars for the detection of faint signals from a stochastic gravitational wave background. Investigating potential causes of magnetospheric changes is crucial when aiming to correct for timing

variability.

Cordes & Shannon (2008) describe the process by which asteroids, formed from supernova fallback material, may enter the magnetosphere of a pulsar and affect both the pulse profile and $\dot{\nu}$. Further evidence for planetary and disk systems around neutron stars is described in Shannon et al. (2013) and references therein. Shannon et al. show that the timing of PSR B1937+21 is consistent with the presence of an asteroid belt. They also refer to other examples of planetary and disk systems around neutron stars, such as the planets around PSR B1257+12 (Wolszczan & Frail 1992) and PSR B1620-26 (Thorsett et al. 1999), the dust disk around magnetar 4U 0142+61 (Wang et al. 2006), and the unusual γ -ray burst GRB 101225A, thought to be due to a minor body falling onto a neutron star (Campana et al. 2011). Also of interest is their reference to circumstantial evidence for asteroid belts around white dwarfs, suggesting that rocky bodies may exist around post main sequence stars.

PSR J0738–4042 is a bright, radio-emitting neutron star with rotational properties similar to the main population of middle-aged, isolated, radio pulsars. It has ν and $\dot{\nu}$ values of approximately 2.667 s^{-1} and $-1.15 \times 10^{-14} \text{ s}^{-2}$ respectively. This pulsar has been the target of a long-term and high-cadence monitoring campaign at the Hartebeesthoek Radio Astronomy Observatory (HartRAO) in South Africa, and a more recent campaign at the Parkes radio telescope in Australia. The result is a unique 24-year dataset in which we have discovered a short period of significant perturbations in $\dot{\nu}$ that coincide with the appearance of a new component in the average pulse profile, first noted by Karastergiou et al. (2011). In section 2, we provide details about the observations of PSR J0738-4042. In section 3, we present the emission and timing variability observed. The data reveal the abrupt changes in rotational stability and emission properties, which have previously only been theoretically predicted as consequences of a pulsar-asteroid encounter (Cordes & Shannon 2008), an interpretation which we discuss in detail in section 4.

2. Observations

Data from PSR J0738–4042 were collected from September 1988 to September 2012 using the 26 m antenna of HartRAO. Observations were made at intervals from 1 to 14 days using receivers at 1600 MHz (1664 and 1668 MHz) or 2300 MHz (2270 and 2273 MHz). The 1600 MHz data have been used here for the profile stability analysis, whereas both data sets were used to obtain timing results. The observations were made of a single polarization: left hand circular. However, the degree of circular polarization in this pulsar is low (Karastergiou et al. 2011), resulting in a negligible difference between true total power profiles and the HartRAO data. During this period the backend provided a single frequency

channel of 10 MHz (until April 2003) and then of 8 MHz at 1600 MHz and of 16 MHz at 2300 MHz. Dispersion due to the interstellar medium is limited to ~ 3 ms across a 10 MHz band centred at 1600 MHz. Observations usually consisted of three consecutive 15 minute (2400 pulsar period) integrations, each resulting in a single integrated profile. There is a gap in the regular coverage from April 1999 - August 2000 (MJD 51295 - 51775) due to equipment upgrade. In order to determine the pulse time of arrival at each epoch, an analytic profile consisting of three Gaussian components was fitted to the integrated profiles. The arrival times were then processed using **TEMPO2** (Hobbs et al. 2006).

Since 2007, PSR J0738–4042 has been observed on a roughly monthly basis at 1369 MHz with the Parkes radio telescope as part of the Fermi timing programme (Weltevrede et al. 2010). The data were recorded with one of the Parkes Digital Filterbank systems (PDFB1/2/3/4) with a total bandwidth of 256 MHz in 1024 frequency channels. Observations are calibrated for differential gain and phase between the feeds using measurements of a noise diode coupled to the receptors in the feed. To correct for cross-coupling of the receptors in the Multibeam receiver, a model of the Jones matrix was used for the receiver computed by observation of the bright pulsar PSR J0437–4715 over the entire range of hour angles visible, using the measurement equation modelling technique (van Straten 2004).

3. Variability in PSR J0738-4042

The radio emission and timing history of PSR J0738–4042 between 1988 and 2012 are presented in Figure 1. To emphasize the variability of the average pulse profile, we have subtracted a constant model profile from each observation. Panel F shows the residual between the data and the model as a function of epoch and rotational pulse phase, centred around the pulse peak and with a temporal resolution of ~ 1.46 ms. After 2008, the observations have a much higher signal-to-noise ratio (S/N), reflecting the higher sensitivity of the Parkes telescope. Each profile included in the HartRAO section of panel F is an average of 8 consecutive observations, in order to increase the S/N. To obtain profiles evenly spaced in time, we averaged 8 profiles per 10-day interval. If a given 10-day interval contained fewer than 8 observations, it was extended by 10 days until 8 profiles could be averaged. This average profile was then used for both 10-day intervals from which the data were taken. The averaging process was not repeated for the Parkes data. However, the data were still divided into 10-day windows, to maintain the same sampling as for HartRAO. If multiple observations existed in a single window, the profile with the highest S/N was used. If no observations existed within a given 10-day window, the profile from the previous window was carried over. We have divided the data into five intervals with distinct profile

shapes, shown in panels A–E. The history of $\dot{\nu}$, computed at 25-day intervals, is plotted in panel G. A dramatic change in pulse shape occurs simultaneously with an abrupt change

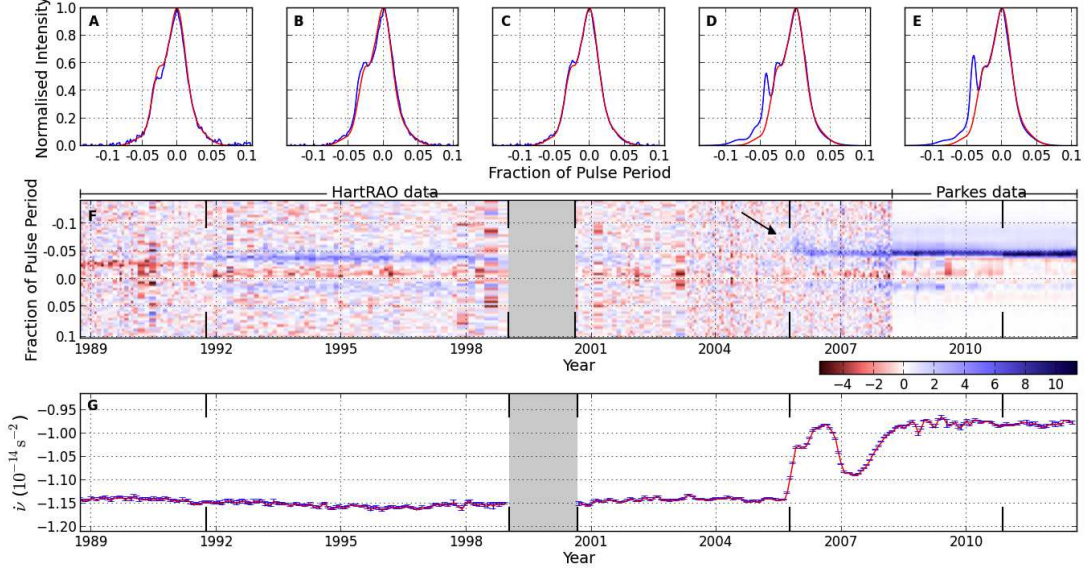


Fig. 1.— Variations in the profile shape and spin-down rate seen in PSR J0738–4042. Profiles are observed at 1600 MHz with HartRAO and at 1369 MHz with the Parkes telescope. Panels A–E: The blue trace denotes the median pulse profile for each of 5 intervals over the 24-year dataset, which are demarcated in panels F and G. The red trace in each plot is a constant model profile which represents the median profile for all of the HartRAO data. Panel F: Map showing the difference between data and the constant model, in units of the HartRAO off-pulse standard deviation. The epochs at which data were collected from both telescopes were used to normalize the Parkes data to the HartRAO scale. The arrow points to drifting emission changes which precede the emergence of a new persistent profile component. Panel G: The pulsar spin-down rate as a function of time.

in torque from September 2005. This change is accompanied by a radio component that initially drifts with respect to the rest of the pulse, before becoming the stable new profile feature reported by Karastergiou et al. (2011). The drifting feature and its relationship with $\dot{\nu}$ are shown in high contrast in Figure 2. Here, $\dot{\nu}$ is interpolated using a non-parametric model, thus avoiding the requirement to choose an explicit functional form for the interpolation (Rasmussen & Williams 2006; Roberts et al. 2012). The drift occurs over ~ 0.02 of the pulse period and has a duration of ~ 100 days. As it begins, a pronounced change in $\dot{\nu}$ is

simultaneously seen in the interpolated curve. The value of $\dot{\nu}$ is relatively stable both before the 2005 event, at $\sim -1.14 \times 10^{-14} \text{ s}^{-2}$ and ~ 1000 days later at $\sim -0.98 \times 10^{-14} \text{ s}^{-2}$.

For the timing analysis presented here, the pulsar times-of-arrival were computed by a standard technique of cross-correlating the observed profile with a template. The template does not include the new component for the HartRAO data, while it does for Parkes. Values of $\dot{\nu}$ were then determined from the times-of-arrival at various observing frequencies: 1600 MHz and 2300 MHz at HartRAO and 1369 MHz at Parkes. The values were calculated using the *glitch* plugin to **TEMPO2**. Overlapping regions of 150 days were selected at 25 day intervals and a timing model of ν and $\dot{\nu}$ was fitted within each region. Values of $\dot{\nu}$ with uncertainties in excess of 10^{-16} s^{-2} , were considered unreliable and not included in Figure 1.

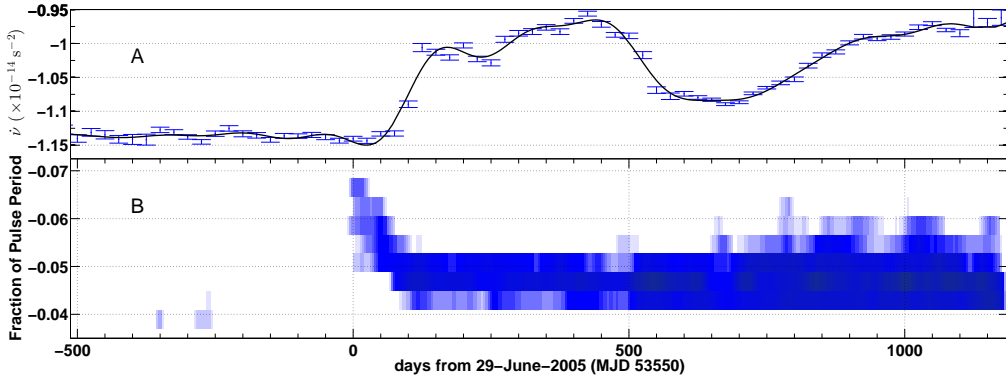


Fig. 2.— Panel A: $\dot{\nu}$ as a function of time, as computed over a 1700 day period referenced to 29 June 2005. The curve is interpolated from data points on which it is overlaid. Panel B: The profile residuals as they appear over the same time period. High contrast is used in order to emphasize the drifting feature.

4. Interpretation and discussion

In considering the source of the variations in magnetospheric currents, which result in the observed $\dot{\nu}$ changes and simultaneous changes in pulse profile, the possibility that PSR J0738–4042 encountered an asteroid or debris from a disk must be explored. Cordes & Shannon (2008), discuss how asteroids, formed from supernova fallback material, may enter the magnetosphere of a pulsar as a result of the migration due to collisions, orbital perturbations and the Yarkovsky effect, or by direct injection from eccentric orbits. A small body, falling towards a pulsar, is evaporated and ionized via pulsar radiation. The remaining charges,

which are electrically captured by gap regions, can perturb particle acceleration in various ways. When accelerated to relativistic energies, charges can produce gamma-rays, which give rise to a pair-production cascade. A quiescent region of the magnetosphere can be activated in this way, leading to new observable emission components. The injected charged particles may also diminish the electric field of a gap region, consequently attenuating an existing pair-production cascade. In the canonical pulsar, radio emission generated at higher altitudes on a set of dipolar magnetic field lines will be beamed at larger angles with respect to the magnetic axis than emission at lower altitudes. Two interpretations of the drift shown in Figure 2 are either azimuthal movement of an emitting region at a given height, or an emission region moving in height along particular magnetic field lines. In the context of the former, the low rate of phase drift does not correspond to any process known, or seen previously in other pulsars (Weltevrede et al. 2006). Additionally, Cordes & Shannon note that a change in pair production can result in a change in emission altitude for a given frequency, due to the plasma frequency dependence on height. We hypothesize hereafter that the phase drift is attributed to a decrease in emission height.

In the case of a dipolar magnetic field emitting over multiple heights, there is a relationship between the angular radius of the field lines ρ at a given height and the observed pulse phase of the emission ϕ ; the lower the altitude, the closer the emission component will be to the centre of the profile. This relationship can be derived using:

$$\sin^2\left(\frac{W}{4}\right) = \frac{\sin^2(\rho/2) - \sin^2(\beta/2)}{\sin \alpha \sin(\alpha + \beta)}, \quad (1)$$

where α is the angle of the magnetic axis with respect to the rotation axis, β is the closest approach of the line of sight to the magnetic axis and W is the total width of the pulse profile (Gil et al. 1984). The observed pulse phase ϕ , measured from the peak of the profile, can be substituted directly for $W/2$. The values of ϕ at which the drift begins and ends are measured in degrees to be $\sim 23.4^\circ$ and $\sim 16.2^\circ$ respectively. In order to obtain a value for ρ , at the beginning and end of the drift (ρ_{begin} and ρ_{end}), α and β for the pulsar are needed. A value for β is obtained via the following equation:

$$\beta = \sin^{-1}\left(\frac{\sin \alpha}{|d\chi/d\phi|_{max}}\right), \quad (2)$$

where $|d\chi/d\phi|_{max}$ is the maximum rate of change of the polarization position angle occurring around the centre of the pulse profile (Rankin 1993). For PSR J0738–4042, $|d\chi/d\phi|_{max}$ is ~ 3 (Karastergiou et al. 2011). The value for α is not easily constrained. Through calculations for various possible values of α , we find that ρ_{begin}/ρ_{end} is largely independent of α . For emission originating close to the magnetic axis, ρ is related to the height H in the following

way (Karastergiou & Johnston 2007):

$$\rho \sim \sqrt{\frac{9\pi H}{2cP}} \quad (3)$$

and therefore,

$$\frac{H_{begin}}{H_{end}} = \left(\frac{\rho_{begin}}{\rho_{end}} \right)^2. \quad (4)$$

As ρ_{begin}/ρ_{end} is insensitive to α , so too is H_{begin}/H_{end} which has a value of ~ 1.5 . The conclusion, therefore, is that the change in height of the drifting emission region is around half of its final emission height.

A reconfiguration in current within a pulsar magnetosphere would simultaneously affect the braking torque and, therefore, the spin-down rate of the pulsar. The 2005 change in $\dot{\nu}$ can be interpreted as a reduction in the total outflowing plasma above the polar caps. The magnitude of the current change, can be inferred from the change in $\dot{\nu}$ following Kramer et al. (2006). The difference between the two extreme $\dot{\nu}$ values corresponds to a reduction in the charge density ρ of $\sim 7 \times 10^{-9} \text{ C cm}^{-3}$, where $\rho = 3I\Delta\dot{\nu}/R_{pc}^4 B_0$, the moment of inertia I is taken to be 10^{45} g cm^2 , the magnetic field $B_0 = 3.2 \times 10^{19} \sqrt{-\dot{\nu}/\nu^3} \text{ Gauss}$, polar cap radius $R_{pc} = \sqrt{2\pi R^3 \nu/c}$ and where the neutron star radius R is taken to be 10^6 cm . We can relate the difference in charge density associated with the two spin-down states to mass supplied to the pulsar, by multiplying it by the speed of light, the polar cap area and the duration of the new spin-down state. Between 2005 and today, this amounts to $\sim 10^{15} \text{ g}$, which lies within the range of known solar system asteroid masses, and is consistent with the mass range of asteroids around neutron stars proposed by Cordes & Shannon (2008). This line of reasoning provides us with a testable hypothesis; at the point in time when the injected mass is exhausted, we would expect the pulsar to return to its previous spin-down state.

If we are witnessing an encounter between the pulsar and an asteroid, the question arises as to whether and why an event would be unique. Although the largest emission and $\dot{\nu}$ change in PSR J0738–4042 occur in 2005, Figure 1 shows a similar but less pronounced emission increase in 1992 along the leading edge of the pulsar. Figure 1 also shows that in 2010, the new component experiences significant and sudden growth, seen clearly in panels D and E. Neither the 1992 or the 2010 emission changes are accompanied by significant $\dot{\nu}$ changes. We also note the multiple profile modes of PSR J0738–4042, as opposed to the seemingly bimodal nature of the state-switching pulsars in Lyne et al. (2010).

The 1992 and 2010 emission changes could also be caused by material entering the magnetosphere, but the smaller effect on pulse profile and the apparent stability of $\dot{\nu}$ during the emission changes may suggest smaller amounts of in-falling matter. The profile changes could be due to a large orbiting body, such as a planet, which periodically disrupts debris in

the fallback disk and precipitates inward migration. As an initial test of this hypothesis, we have simulated the perturbation to timing measurements of this pulsar by an orbiting planet. We performed a periodicity analysis of the residuals in 1000 day segments, using the Cholesky pre-whitening method of Coles et al. (2011) and fitting for sinusoids with frequencies linearly spaced from 0.001 per day to 10 per day. We then computed a weighted mean of the resulting periodograms. Using a 5σ threshold we found no significant signals at long periods, and only two significant periodic signals, at exactly 1 per day and 2 per day, the origin of which is unclear. By injecting a simulated planetary signature with a circular orbit of radius 10^9 m (typical gravitational tidal radius (Cordes & Shannon 2008)) we rule out any such planet with mass greater than 6×10^{28} g. A planet of smaller mass may, therefore, exist without imprinting its signature on the timing data of this pulsar. As a future step, we intend to test the idea of periodic disruption of a debris disk by a planet, by monitoring PSR J0738–4042 for years to come, to see whether the emission profile and $\dot{\nu}$ will periodically vary.

The investigation of alternative interpretations, and glitches in particular, forms part of our future plans. The observed emission variability and rotational instabilities of magnetars are of interest in this context, especially given the latest estimates of the surface magnetic field of SGR 0418+5729 (Rea et al. 2013), which provides a link between the high magnetic field neutron stars and radio pulsars. Variability may prove to be another common characteristic between these populations of neutron stars.

The Parkes radio telescope is part of the Australia Telescope National Facility which is funded by the Commonwealth of Australia for operation as a National Facility managed by CSIRO. Data taken at Parkes is available via a public archive. Consult the web page <http://www.atnf.csiro.au/research/pulsar/index.php?n=Main.ANDSATNF> for details. P.R.B. is grateful to the Science and Technology Facilities Council and CSIRO Astronomy and Space Science for support throughout this work. We thank the referee Scott Ransom for valuable comments that helped to improve the text.

REFERENCES

- Camilo, F., Cognard, I., Ransom, S. M., et al. 2007, *ApJ*, 663, 497
- Camilo, F., Ransom, S. M., Chatterjee, S., Johnston, S., & Demorest, P. 2012, *ApJ*, 746, 53
- Campana, S., Lodato, G., D’Avanzo, P., et al. 2011, *Nature*, 480, 69
- Coles, W., Hobbs, G., Champion, D. J., Manchester, R. N., & Verbiest, J. P. W. 2011, *MNRAS*, 418, 561

- Cordes, J. M., & Shannon, R. M. 2008, *ApJ*, 682, 1152
- Edwards, R. T., Hobbs, G. B., & Manchester, R. N. 2006, *MNRAS*, 372, 1549
- Gil, J., Gronkowski, P., & Rudnicki, W. 1984, *A&A*, 132, 312
- Hobbs, G. B., Edwards, R. T., & Manchester, R. N. 2006, *MNRAS*, 369, 655
- Wang, N., Manchester, R. N., Zhang, J., et al. 2001, *MNRAS* 328, 855
- Karastergiou A., Roberts, S. J., Johnston, S., et al. 2011, *MNRAS*, 415, 251
- Karastergiou, A., & Johnston, S. 2007, *MNRAS*, 380, 1678
- Keith, M. J., Shannon, R. M., & Johnston, S. 2013, *MNRAS*, 423, 3080
- Kramer, M., Lyne, A. G., O’Brien, J. T., Jordan, C. A., & Lorimer, D. R. 2006, *Science*, 312, 549
- Lorimer, D. R., Lyne, A. G., McLaughlin, M. A., et al. 2012 *ApJ*, 758, 141
- Lyne, A., Hobbs, G., Kramer, M., Stairs, I., & Stappers, B. 2010, *Science*, 329, 408
- Rankin, J. M. 1993, *ApJ*, 405, 285
- Rasmussen, C. E., & Williams, C. K. I. 2006, *Gaussian Processes for Machine Learning*, The MIT Press
- Rea, N., Israel, G. L., Pons, J. A., et al. 2013, *ApJ*, 770, 65
- Roberts, S., Osborne, M., Ebdem, M., et al. 2012, *Phil. Trans. R. Soc. A*, 371
- Shannon, R. M., Cordes, J. M., Metcalfe, T. S., et al. 2013, *ApJ*, 766, 5
- Thorsett, S. E., Arzoumanian, Z., Camilo, F., & Lyne, A. G. 1999, *ApJ*, 523, 763
- Timokhin, A. N. 2010, *MNRAS*, 408, L41
- van Straten, R. N. 2004, *ApJS* 152, 129
- Wang, Z., Chakrabarty, D., & Kaplan, D. L. 2006, *Nature*, 440, 772
- Weltevrede, P., Edwards, R. T., & Stappers, B. W. 2006, *A&A*, 445, 243
- Weltevrede, P., Johnston, S., Manchester, R. N., et al. 2010, *Proc. Astr. Soc. Aust.*, 27, 64
- Weltevrede, P., Johnston, S., & Espinoza, C. M. 2011, *MNRAS*, 411, 1917

Wolszczan, A., & Frail, D. A. 1992, *Nature*, 355, 145

Woods, P. M., & Thompson, C. 2006, in *Compact Stellar X-Ray Sources*, ed. W. H. G. Lewin & M. van der Klis (Cambridge: Cambridge Univ. Press), 547